Interfacial charge transfer and electronic structure of diamond/c-BN heterointerface

Suna Jia[1,2], Shiyang Fu[1,2], Yaning Liu[1,2], Nan Gao[1,2]*, Hongdong Li[1,2]*, Meiyong Liao[3]

[1]*State Key Lab of Superhard Materials, College of Physics, Jilin University, Changchun 130012, P. R. China*

[2]*Shenzhen Research Institute, Jilin University, Shenzhen 518057, P. R. China*

[3]*Research Center for Functional Materials, National Institute for Materials Science (NIMS), Tsukuba Ibaraki, 305-0044, Japan*

Abstract

In this work, the interfacial structures and electronic properties of diamond and cubic boron nitride heterostructures are investigated using first principles calculation. It is found that the two-dimensional electron (hole) gas appears in diamond surface for structures with interface C-N (C-B) bonds, while the doping type is not related to the crystal orientation and surface fictionalization. The areal electron (hole) density values are 6.57×10^{13}–1.57×10^{14} cm^{-2} (2.24×10^{14}–3.72×10^{14} cm^{-2}), which is slightly larger than the areal hole density in hydrogen-terminated diamond. This work is helpful for promoting diamond applied in electronic and opto-electronic devices.

Keywords: diamond, cubic boron nitride, heterointerface, interfacial charge transfer, first principles calculation

Corresponding Authors

Email address: gaon@jlu.edu.cn, hdli@jlu.edu.cn

1. Introduction

As an ultra-wide band gap semiconductor, diamond has attracted extensive attention due to its exciting properties in physics, devices and applications.[1] Although the *p*-type and *n*-type diamonds have been obtained by the conventional doping method, the foreign atoms incorporate into diamond to form the electrically active dopants are limited.[2,3] Besides, the diamond surface with hydrogen (H) termination shows the two-dimensional hole gas, which is explained by the surface charge transfer doping mechanism,[4] and the field effect transistors based on the H-terminated diamond have been realized.[5]

The cubic boron nitride (c-BN) has high thermal and chemical stabilities, and it is promising for high-power electronic devices.[6] Since the lattice parameter of c-BN is good matched with diamond, it is selected as a substrate to grow the c-BN single crystal, using a temperature gradient method at high temperature and high pressure,[7] the dual ion-beam sputtering,[8,9] ion-beam-assisted molecular beam epitaxy[10-12] and ion-beam-assisted deposition methods.[9] The epitaxial (111)[7,10] diamond and c-BN (D/BN) heterojunction was obtained. However, the poor crystal quality of heterojunction makes it difficult to directly image the interface structures and measure the electronic properties, which is fundamental to designing optimal synthesis routes, and it is also essential for applications in nanodevices.

The previous theoretical works were devoted to calculate the band edge discontinuities[13,14] and the valence band offset[15,16] of D/BN interfaces. In order to provide more fundamental information, herein, we systemically investigate the interface structures and electronic properties of (100), (110) and (111) D/BN heterointerfaces using first principles calculation. It is found the two-dimensional electron (hole) gas for heterostructures with interface C-N (C-B) bonds.

2. Calculation details

The geometrical optimizations and electronic property calculations were carried out using the density functional theory (DFT) as implemented in the Vienna ab initio simulation package (VASP).[17,18] The exchange-correlation potential was treated by means of Perdew-Burke-Ernzerh (PBE) under the framework of generalized gradient approximation (GGA).[19] The projector augmented wave (PAW) method was used to describe the electron-ion interaction.[20]

A plane wave kinetic energy cut-off was set as 600 eV. In the geometrical optimizations and density of state (DOS) calculations, the *k*-point meshes were 5 × 5 × 1 and 10 × 10 × 1, respectively. The geometrical optimizations using the conjugate gradient method were completed until the convergence tolerance of energy was smaller than 10^{-5} eV, and the force was smaller than 0.03 eV/Å. A large vacuum of 30 Å in the *z*-direction was used to eliminate the interaction between the periodic images.

3. Results and discussion

The lattice constants of bulk diamond and c-BN are calculated as 3.572 Å and 3.626 Å, respectively, being similar with the experimental results of 3.567 Å[21] and 3.615 Å.[22] To build the heterostructure, lattice constant of c-BN is shrunken by 1.51% to match that of diamond. Based on the previous results,[23] the smooth interface is built for D/BN heterostructures.

The (111) and (100) D/BN heterostructures are first studied. The H-terminated c-BN surface can be accessibly obtained by the microwave H-plasma treatment,[24] thus both pristine and hydrogenated c-BN surfaces are considered. Four kinds of stable c-BN (111) surfaces are reported in our previous work,[25] including the pristine and hydrogenated (2×1) c-BN, hydrogenated (1×1) c-BN surface with B-termination and N-termination. The (111) D/BN heterostructures are shown in FIG. 1(a)-1(d), which are named from (111)-I to (111)-IV structures, respectively. For c-BN (100) surface, the (2×1) reconstructed surfaces with B-B and N-N dimers are stable.[26] Then, the pristine and hydrogenated c-BN (100) surfaces with dimers are considered. The (100) D/BN heterostructures are presented in FIG. 1(e)-1(h), being defined as (100)-I to (100)-IV structures, respectively. To avoid the appearance of irrelevant surface states in band structure for polar semiconductor surface,[27,28] the B and N atoms on the hydrogenated c-BN surface are saturated by appropriate fractionally charged H atoms.

Also, two types of atoms in c-BN offer the possibility of forming the structures with interface C-N bonds (group 1: (111)-I, (111)-II, (111)-III, (100)-I, (100)-II structures) and interface C-B bonds (group 2: (111)-IV, (100)-III, (100)-IV structures). Although the experimental works reported the formation of C-B bonds at the interface for the diamond and c-BN heterostructure in the transmission electron microscopy studies.[7,10] Another work

suggested a C-N interface after the comparison with offsets predicted by theoretical calculations.[29] Also, both C-N and C-B bonds appear in carbon and BN heteronanotubes[30,31] and hydrogenated graphene and BN heterostructures.[32] Thus, the heterostructures with interface C-N and C-B bonds are investigated in this work.

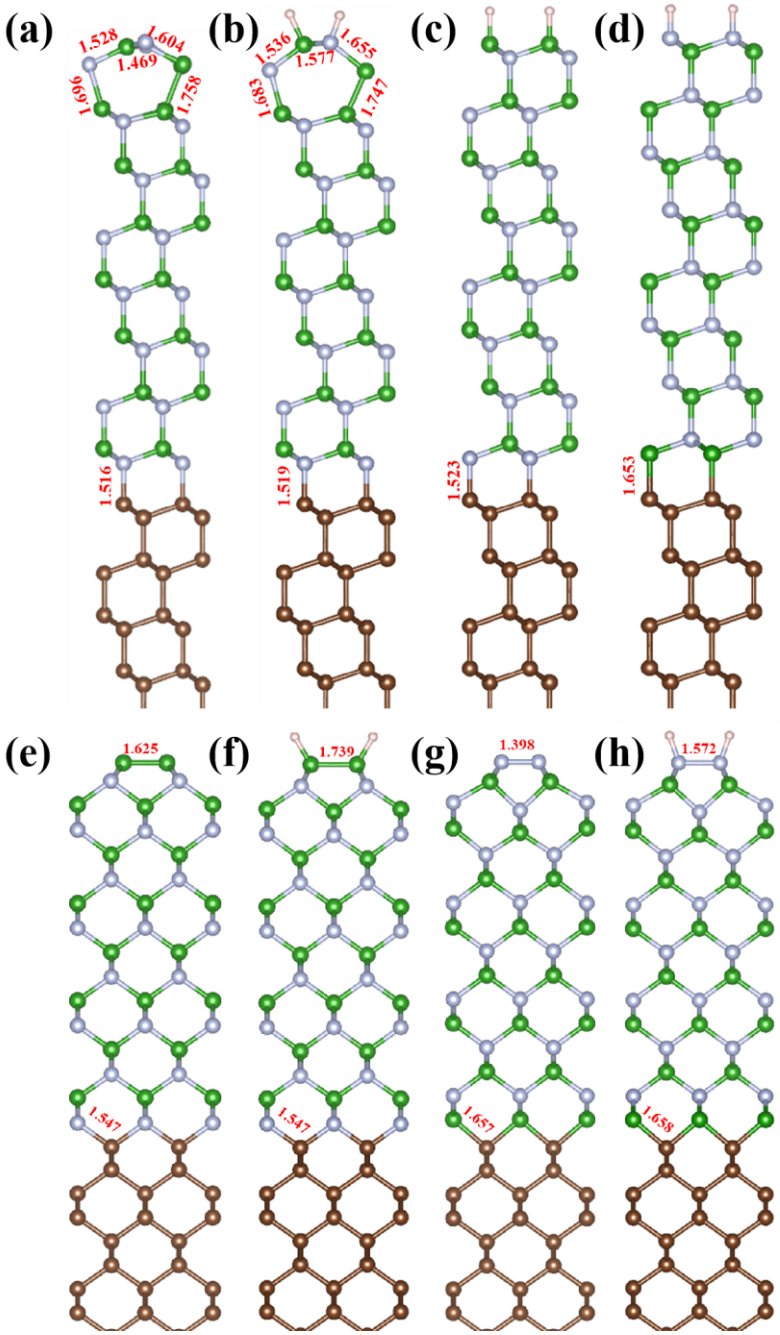

FIG. 1. The side views of (111) and (100) D/BN heterostructures after geometrical optimization for (a) (111)-I, (b) (111)-II, (c) (111)-III, (d) (111)-IV, (e) (100)-I, (f) (100)-II, (g) (100)-III, (h) (100)-IV structures. The interface and partial surface bond lengths are labeled. The brown, green, grey and pink balls are C, B, N and H atoms, respectively.

The surface B-N and B-B bond lengths for the (111)-I and (111)-II heterostructures are similar with those in the reconstructed c-BN (111) surface.[25] For (100) D/BN heterointerfaces, the surface B-B and N-N bonds length ($l_{B\text{-}B}$ and $l_{N\text{-}N}$) are 1.625 Å and 1.398 Å for the pristine (2×1) structures, and 1.739 Å and 1.572 Å for hydrogenated surfaces. The former values are approaching to those (1.63 Å and 1.55 Å) in pristine c-BN (100) surface.[26,33] After geometrical optimization, the structural parameters are list in Table 1, it is found that the slight structural distortion occurs in the diamond and c-BN interface. The interface C-N bond lengths ($l_{C\text{-}N}$) of (111)-I, (111)-II, (111)-III structures are 1.516–1.523 Å, and those for (100)-I, (100)-II structures are 1.547 Å. The interface C-B bond lengths ($l_{C\text{-}B}$) are 1.653 Å for (111)-IV structure, and 1.657–1.658 Å for (100)-III, (100)-IV structures. It denotes the formation of strong covalent bonds in the interface between diamond and c-BN. The interface $l_{C\text{-}N}$ and $l_{C\text{-}B}$ values for (111)-III and (111)-IV structures are approaching to those (1.524 Å and 1.650 Å) in a previous work.[14]

The band structures of (111) and (100) D/BN heterostructures are presented in FIG. 2. For structures in group 1 those with interface C-N bonds, there are several conductance bands crossing the Fermi level, suggesting that the surface *n*-type conductivity appears. For structures (group 2) with interface C-B bonds, the valence bands cross the Fermi level, denoting the *p*-type doping characteristic. The similar electronic feature for (111)-III and (111)-IV structures has been observed in previous theoretical predictions.[7,14] Due to the strong interface interaction between the diamond and c-BN, it is naturally supposed that the surface conductivity in D/BN heterointerface should be thermally stable up to a higher temperature compared with the H-terminated diamond.[4,34]

We plot the charge density figures for the bands near the Fermi energy for each structure in FIG. S1. There are several flat bands near the Fermi energy for the heterostructures with pristine surface (conductance bands for (111)-I structure, and valence bands for (100)-I and (100)-III structures). The flat bands are mainly contributed by the surface atoms, and the surface states disappear after surface functionalization ((111)-II, (100)-II and (100)-IV structures). Comparing the conductance bands crossing the Fermi energy for (111)-I, (111)-II, (111)-III, (100)-I and (100)-II structures, except the bands contributed by the surface atoms in

c-BN surface, the conductance bands are contributed by the diamond and c-BN interface. This phenomenon is also observed in the valence bands crossing the Fermi energy for (111)-IV, (100)-III and (100)-IV structures. It is concluded that the surface functionalization has little effect on the doping characteristic, while it is determined by the interface between diamond and c-BN.

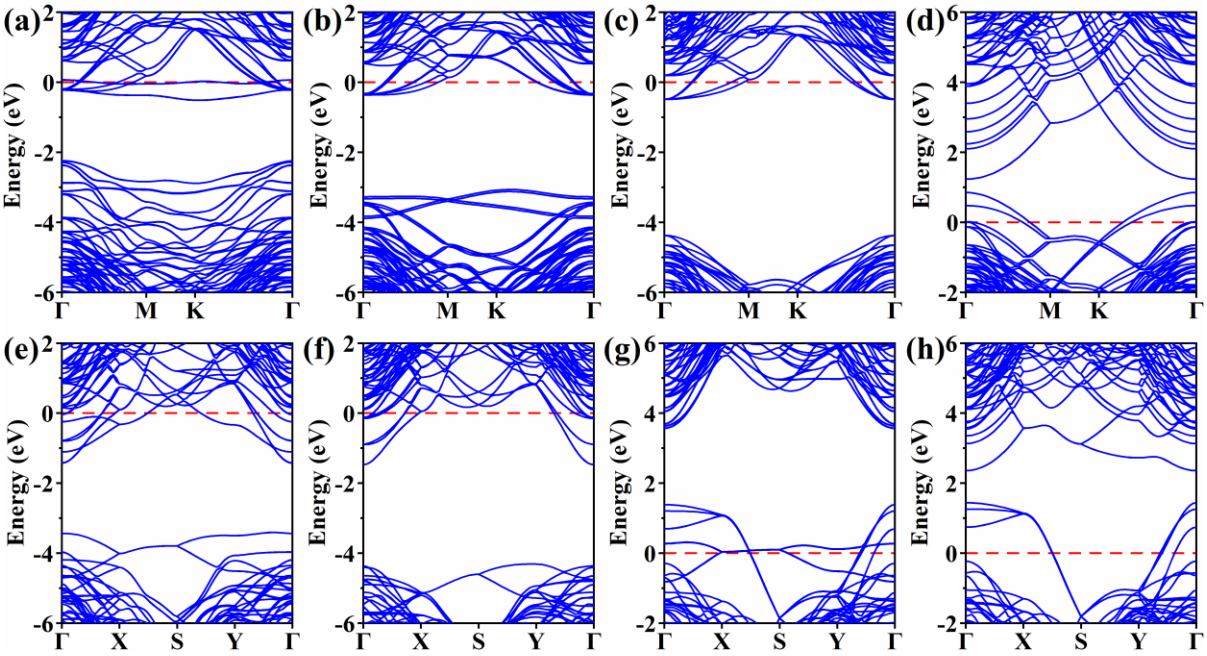

FIG. 2. The band structures of D/BN heterostructures for (a) (111)-I, (b) (111)-II, (c) (111)-III, (d) (111)-IV, (e) (100)-I, (f) (100)-II, (g) (100)-III, (h) (100)-IV structures. The Fermi energy is set at zero.

The DOS of (111) and (100) D/BN heterostructures in FIG. 3 confirm the *n* (*p*) type doping feature for group 1 (2) structures with interface C-N (C-B) bonds. For group 1, we integrate the partial DOS of conductance band for diamond to obtain the areal electron densities of 6.57 × 10^{13} cm^{-2}, 7.94 × 10^{13} cm^{-2}, 9.45 × 10^{13} cm^{-2}, 1.57 × 10^{14} cm^{-2}, 1.55 × 10^{14} cm^{-2} for (111)-I, (111)-II, (111)-III, (100)-I, (100)-II structures, respectively. For group 2, we integrate the partial DOS of valence band for diamond to get the areal hole densities of 2.24 × 10^{14} cm^{-2}, 3.33 × 10^{14} cm^{-2}, 3.72 × 10^{14} cm^{-2} for (111)-IV, (100)-III, (100)-IV structures. The areal hole density for D/BN heterostructure is slightly larger than that for H-terminated diamond (~10^{13} cm^{-2}).[4]

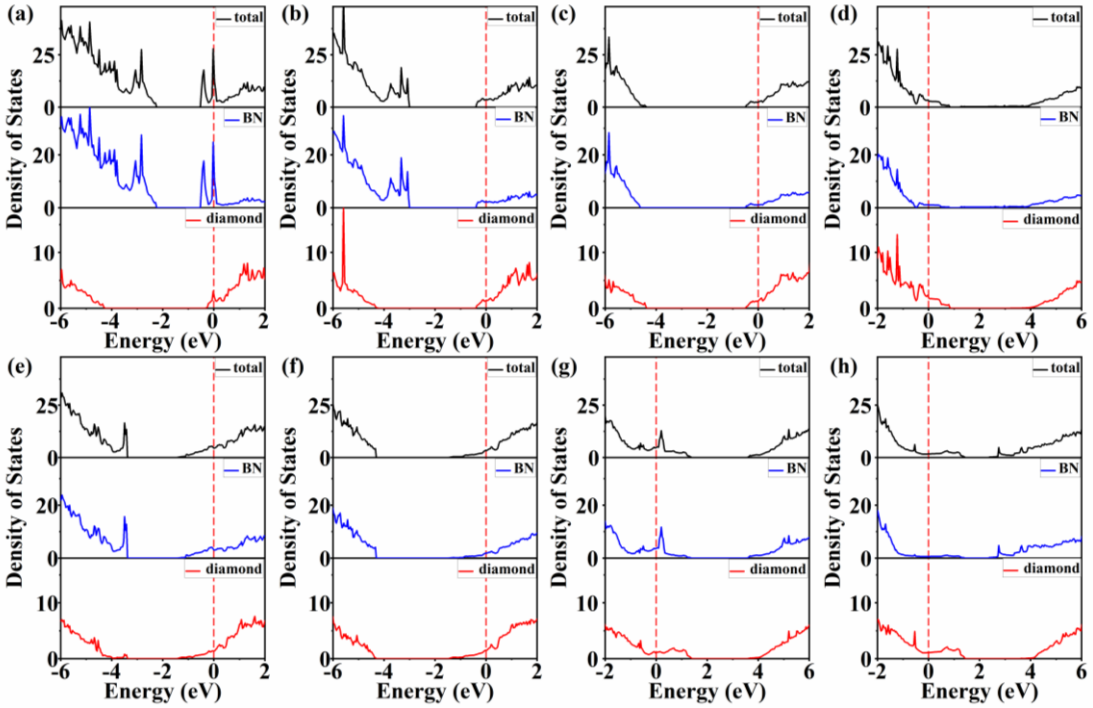

FIG. 3. The DOS of D/BN heterostructures for (a) (111)-I, (b) (111)-II, (c) (111)-III, (d) (111)-IV, (e) (100)-I, (f) (100)-II, (g) (100)-III, (h) (100)-IV structures. The Fermi energy is set at zero.

We further plot the charge density difference plots for D/BN heterostructures in FIG. 4, which is defined as $\Delta\rho = \rho_{total} - \rho_{diamond} - \rho_{BN}$ (ρ_{total}, $\rho_{diamond}$ and ρ_{BN} are the charge density of heterostructure, diamond and c-BN, respectively). There are evidently charge transfer in interface between diamond and c-BN. For group 1 structures, the C atoms in diamond lose electron from N atoms in c-BN, which makes the electron accumulation in the diamond surface. For group 2 structures, the C atoms in diamond surface get electron from interface B atoms in c-BN, then the hole accumulates in diamond surface. Namely, the two-dimensional electron (hole) gas appears in diamond surface for group 1 (2) structures with interface C-N (C-B) bonds. The charge density difference feature is consistent with the Bader charge analysis (Q). The electron of 0.983 e, 0.985 e, 1.085 e, 1.580 e, 1.589 e is lost in diamond surface for group 1 structures, and electron of 1.823 e, 3.426 e, 3.424 e is transferred from c-BN to diamond surface for group 2 structures.

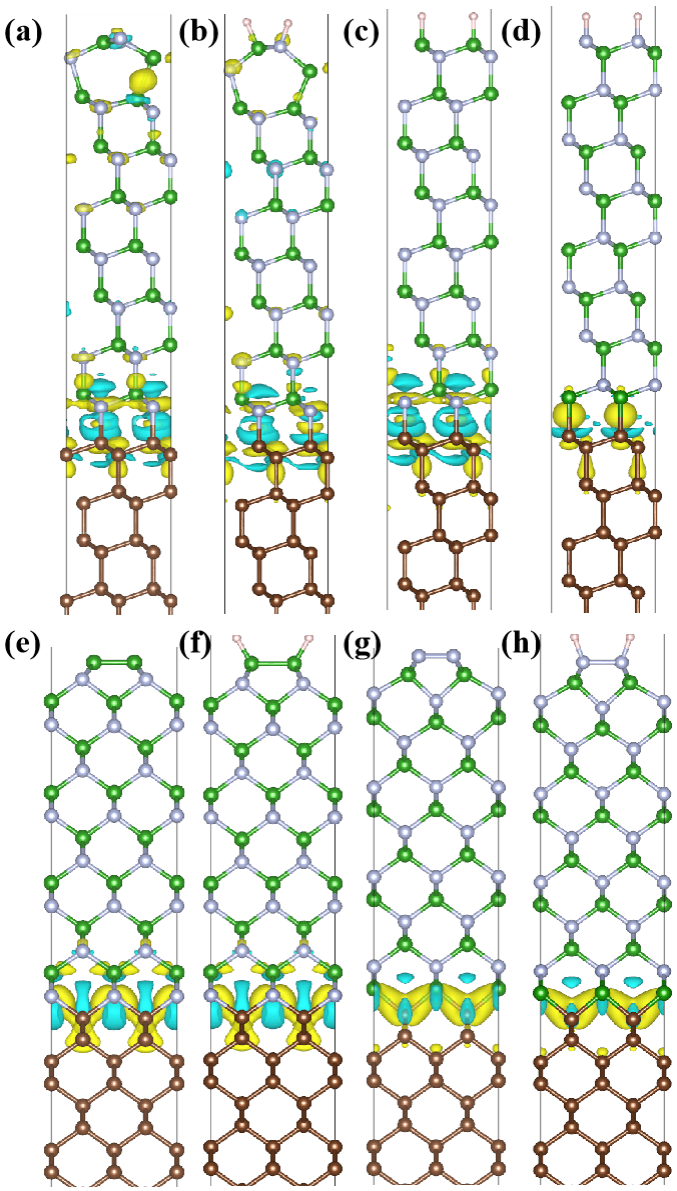

FIG. 4. The charge density difference of D/BN heterostructures for (a) (111)-I, (b) (111)-II, (c) (111)-III, (d) (111)-IV, (e) (100)-I, (f) (100)-II, (g) (100)-III, (h) (100)-IV structures. The yellow (cyan) color represents electron accumulation (depletion). The isosurface value is 0.00036 e/Å^3.

We also build the structural model of (110) D/BN heterointerface, and calculate the band structure. As shown in FIG. 5, the interface of (110) D/BN heterostructure has both C-N and C-B bonds, and the numbers of C-N and C-B bonds in the interface are equal. We find the semiconducting characteristic without doping for (110) D/BN heterostructure. Consequently, the doping type of diamond is not related with the crystal orientation, while it is determined by the interface C-N or C-B bonds.

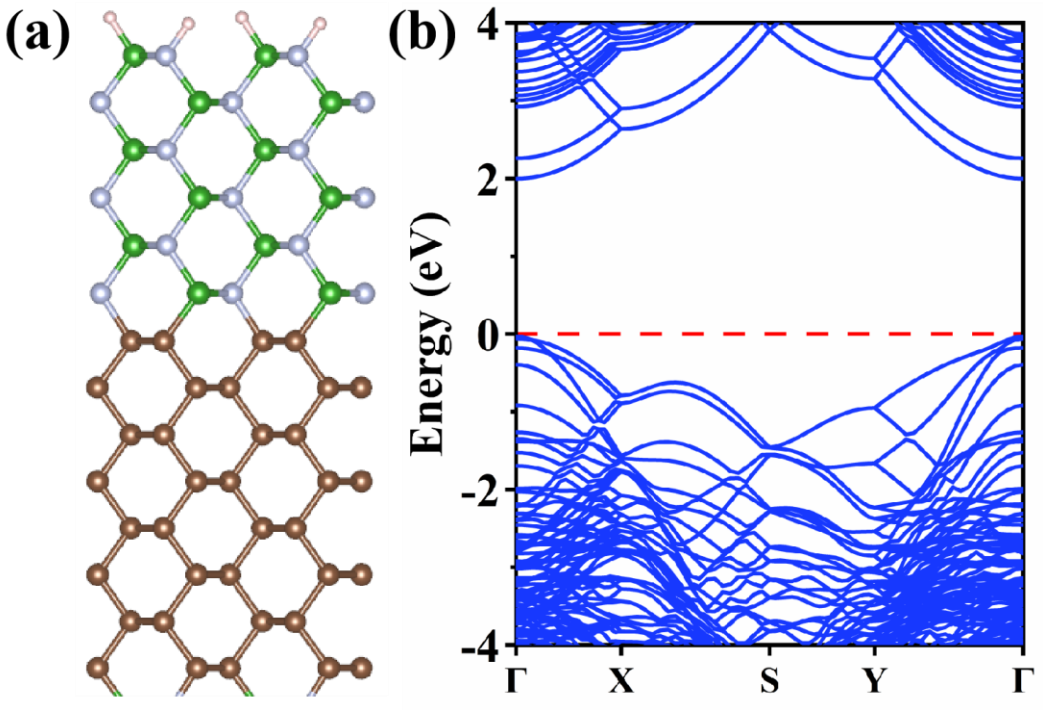

FIG. 5. (a) Side view and (b) band structure of (110) D/BN heterointerface. The green, grey, brown and pink balls represent B, N, C and H atoms, respectively. The Fermi energy is set as zero.

Finally, we calculate the formation energies (E_F) with respect to bulk diamond, c-BN and free H_2 molecule using the following equation:

$$E_F = (E_{C/BN} - n_C\mu_C - n_{BN}\mu_{BN} - n_H\mu_H)/n_{bond}, \quad (1)$$

Where $E_{C/BN}$ is the total energy of the heterostructure, μ_C and μ_{BN} is the energy of individual C atoms and BN units in the bulk material, μ_H is half of the total energy of a single H_2 molecule. n_C, n_{BN} and n_H is the number of C atoms, BN units and H atoms, and n_{bond} is the number of interface bonds. As shown in Table 1, the group 2 structures have smaller formation energy than the group 1 structures, suggesting that the formation of group 2 structures with interface C-B bonds is easier.

Table 1 The structural parameters and electronic properties of (100) and (111) D/BN heterostructures. The interface C-N or C-B bond length (l), charge carried by diamond (Q), areal electron density, areal hole density, and formation energy (E_F).

	Structure	l (Å)	Q (e)	Areal electron density (cm^{-2})	Areal hole density (cm^{-2})	E_F (eV)
Group 1	(111)-I	1.516	0.983	6.57×10^{13}	/	2.959
	(111)-II	1.519	0.985	7.94×10^{13}	/	3.300
	(111)-III	1.523	1.085	9.45×10^{13}	/	1.119
Group 2	(111)-IV	1.653	1.823	/	2.24×10^{14}	0.682
Group 1	(100)-I	1.547	1.580	1.57×10^{14}	/	2.639
	(100)-II	1.547	1.589	1.55×10^{14}	/	1.972
Group 2	(100)-III	1.657	3.426	/	3.33×10^{14}	1.570
	(100)-IV	1.658	3.424	/	3.72×10^{14}	1.587

4. Conclusion

In summary, the interface structures and electronic properties of (100), (110) and (111) D/BN heterointerface are systemically investigated using first principles calculation. The electronic structures of D/BN heterostructure show the interface donor (acceptor) feature, being ascribed to the C-N (C-B) bonds in the interface, while it is not related to the crystal orientation and surface functionalization. The areal electron densities are 6.57×10^{13}–1.57×10^{14} cm^{-2} for structures with interface C-N bonds, and the areal hole densities are 2.24×10^{14}–3.72×10^{14} cm^{-2} for structures with interface C-B bonds. The areal carrier density value is slightly larger than the areal hole density of H-terminated diamond. The charge density difference and Bader charge calculations denote the interfacial charge transfer. The electronic state could be manipulated for advanced electronic device applications.

Acknowledgments

This work was supported by the Key-Area Research and Development Program of Guangdong Province (No. 2020B0101690001), and the National Natural Science Foundation of China (NSFC) (No. 51972135, 52172044). Computation was carried out at the High-Performance Computing Center of Jilin University.

References

[1] O. Madelung, W. Von der Osten, and U. Rössler, Intrinsic Properties of Group IV Elements and III-V, II-VI and I-VII Compounds/Intrinsische Eigenschaften Von Elementen Der IV. Gruppe und Von III-V-, II-VI-und I-VII-Verbindungen, Springer Science & Business Media, Vol. 22 (1986).

[2] M. A. Pinault, J. Barjon, T. Kociniewski, F. Jomard, and J. Chevallier, The n-type doping of diamond: Present status and pending questions, Physica B Condens. Matter **401**, 51 (2007).

[3] H. Yang, Y. Ma, and Y. Dai, Progress of structural and electronic properties of diamond: a mini review, Functional Diamond **1**, 150 (2021).

[4] F. Maier, M. Riedel, B. Mantel, J. Ristein, and L. Ley, Origin of surface conductivity in diamond, Phys. Rev. Lett. **85**, 3472 (2000).

[5] K. G. Crawford, I. Maini, D. A. Macdonald, and D. A. Moran, Surface transfer doping of diamond: A review, Prog. Surf. Sci. **96**, 100613 (2021).

[6] N. Izyumskaya, D. O. Demchenko, S. Das, U. Ozgur, V. Avrutin, and H. Morkoc, Recent Development of Boron Nitride towards Electronic Applications, Adv. Electron. Mater. **3**, 1600485 (2017).

[7] C. Chen, Z. Wang, T. Kato, N. Shibata, T. Taniguchi, and Y. Ikuhara, Misfit accommodation mechanism at the heterointerface between diamond and cubic boron nitride, Nat. Commun. **6**, 1 (2015).

[8] H. Yin and P. Ziemann, Multiple delta doping of single crystal cubic boron nitride films heteroepitaxially grown on (001) diamonds, Appl. Phys. Lett. **104**, 252111 (2014).

[9] X. W. Zhang, H. G. Boyen, P. Ziemann, and F. Banhart, Heteroepitaxial growth of cubic boron nitride films on single-crystalline (001) diamond substrates, Appl. Phys. A **80**, 735 (2005).

[10] K. Hirama, Y. Taniyasu, H. Yamamoto, and K. Kumakura, Structural analysis of cubic boron nitride (111) films heteroepitaxially grown on diamond (111) substrates, J. Appl. Phys. **125**, 115303 (2019).

[11] K. Hirama, Y. Taniyasu, S.-i. Karimoto, H. Yamamoto, and K. Kumakura, Heteroepitaxial growth of single-domain cubic boron nitride films by ion-beam-assisted MBE, Appl. Phys. Express **10**, 035501 (2017).

[12] K. Hirama, Y. Taniyasu, S.-i. Karimoto, Y. Krockenberger, and H. Yamamoto, Single-crystal cubic boron nitride thin films grown by ion-beam-assisted molecular beam epitaxy, Appl. Phys. Lett. **104**, 092113 (2014).

[13] W. E. Pickett, Thin superlattices and band-gap discontinuities: The (110) diamond–boron nitride interface, Phys. Rev. B **38**, 1316 (1988).

[14] D. H. Zhao, W. Gao, Y. J. Li, Y. Y. Zhang, and H. Yin, The electronic properties and band-gap discontinuities at the cubic boron nitride/diamond hetero-interface, RSC Adv. **9**, 8435 (2019).

[15] K. Yamamoto, K. Kobayashi, T. Ando, M. Nishitani-Gamo, R. Souda, and I. Sakaguchi, Electronic structures of the diamond/boron-nitride interface, Diam. Relat. Mater. **7**, 1021 (1998).

[16] H. Guo-min, Z. Yong-mei, W. Ren-zhi, and L. Shu-ping, Stability and electronic structures of the polar diamond/boron-nitride (001) interface, Solid State Commun. **118**, 287 (2001).

[17] Kresse and Furthmuller, Efficient iterative schemes for ab initio total-energy calculations using a plane-wave basis set, Phys. Rev. B **54**, 11169 (1996).

[18] G. Kresse and J. Furthmüller, Efficiency of ab-initio total energy calculations for metals and semiconductors using a plane-wave basis set, Comput. Mater. Sci. **6**, 15 (1996).

[19] J. P. Perdew, K. Burke, and M. Ernzerhof, Generalized gradient approximation made simple, Phys. Rev. Lett. **77**, 3865 (1996).

[20] P. E. Blöchl, Projector augmented-wave method, Phys. Rev. B **50**, 17953 (1994).

[21] L. Bursill, J. Hutchison, N. Sumida, and A. Lang, Measurements of diamond lattice displacement by platelet defects with electron microscopic moiré patterns, Nature **292**, 518 (1981).

[22] P. Mirkarimi, K. McCarty, and D. Medlin, Review of advances in cubic boron nitride film synthesis, Mater. Sci. Eng. R Rep. **21**, 47 (1997).

[23] Z. J. Lin, X. H. Peng, C. Huang, T. Fu, and Z. C. Wang, Atomic structure, electronic properties and generalized stacking fault energy of diamond/c-BN multilayer, RSC Adv. **7**, 29599 (2017).

[24] B. He, T. W. Ng, M. F. Lo, C. S. Lee, and W. J. Zhang, Surface Transfer Doping of Cubic Boron Nitride Films by MoO3 and Tetrafluoro-tetracyanoquinodimethane (F4-TCNQ), ACS Appl. Mater. **7**, 9851 (2015).

[25] Z. L. Sun, N. Gao, and H. D. Li, Structural and electronic properties of c-BN (111) surface with hydrogen/fluorine functionalization and nitrogen-based small-molecule adsorption, J. Phys.: Condens. Matter **32** (2020).

[26] J. Karlsson and K. Larsson, Hydrogen-Induced De/Reconstruction of the c-BN(100) Surface, J. Phys. Chem. C **114**, 3516 (2010).

[27] X. Huang, E. Lindgren, and J. R. Chelikowsky, Surface passivation method for semiconductor nanostructures, Phys. Rev. B **71**, 165328 (2005).

[28] K. Shiraishi, A new slab model approach for electronic structure calculation of polar semiconductor surface, J. Phys. Soc. Japan **59**, 3455 (1990).

[29] J. Shammas, Y. Yang, X. Wang, F. A. Koeck, M. R. McCartney, D. J. Smith, and R. J. Nemanich, Band offsets of epitaxial cubic boron nitride deposited on polycrystalline diamond via plasma-enhanced chemical vapor

deposition, Appl. Phys. Lett. **111**, 171604 (2017).

[30] A. J. Du, Y. Chen, Z. H. Zhu, G. Q. Lu, and S. C. Smitht, C-BN Single-Walled Nanotubes from Hybrid Connection of BN/C Nanoribbons: Prediction by ab initio Density Functional Calculations, J. Am. Chem. Soc. **131**, 1682 (2009).

[31] W. An and C. H. Turner, Linking carbon and boron-nitride nanotubes: Heterojunction energetics and band gap tuning, J. Phys. Chem. Lett. **1**, 2269 (2010).

[32] X. Chen, J. Lian, and Q. Jiang, Band-gap modulation in hydrogenated graphene/boron nitride heterostructures: the role of heterogeneous interface, Phys. Rev. B **86**, 125437 (2012).

[33] J. Widany, F. Weich, T. Köhler, D. Porezag, and T. Frauenheim, Dynamic properties and structure formation of boron and carbon nitrides, Diam. Relat. Mater. **5**, 1031 (1996).

[34] M. Riedel, J. Ristein, and L. Ley, Recovery of surface conductivity of H-terminated diamond after thermal annealing in vacuum, Phys. Rev. B **69**, 125338 (2004).